

Angular analyses of exclusive $\bar{B} \rightarrow X_J \ell_1 \ell_2$ decays for spin $J \leq 4$

Biplab Dey¹

¹*Sezione INFN di Milano, Milano, Italy*

(Dated: September 21, 2016)

As an update to our previous calculation for spin $J \leq 2$, we present the angular moments for exclusive $\bar{B} \rightarrow X_J \ell_1 \ell_2$, where ℓ_1 is a charged massless lepton and ℓ_2 is a charged or neutral massless lepton, and X_J is a mesonic system with spin $J \leq 4$. The expected applications include higher resonances in the $[K\pi]$ system in $\bar{B}^0 \rightarrow K^- \pi^+ \mu^- \mu^+$ at LHCb in Run II, and in the $[\pi\pi]$ system for $\bar{B} \rightarrow \pi\pi \ell^- \bar{\nu}_\ell$ at Belle II. For the $J \leq 2$ case, we also provide a set of consistency relations among the measured moments observables and validate them against the latest measurements from LHCb.

PACS numbers: 12.15.-y, 12.10.Dm, 13.20.-v, 12.15.Hh

I. INTRODUCTION

With the advent of the next generation of B factories at LHCb and Belle II, hitherto rare decays are quickly shedding the “rare” tag. A good example is the flavor changing neutral current decay $\bar{B}^0 \rightarrow \bar{K}^{*0} \mu^- \mu^+$ [1], where the signal yield is expected to reach $\mathcal{O}(10^4)$ after Run II at LHCb. It is therefore pertinent to look beyond the dominant hadronic resonant structures contributing to rare or Cabibbo-suppressed B decays in the electroweak penguin and semileptonic sectors, which, together we classify as $\bar{B} \rightarrow X_J \ell_1 \ell_2$. The hadronic X_J system here is typically $[\pi\pi]$ or $[K\pi]$ and the leptons $\ell_{1,2}$ are assumed massless. The goal of this paper is lay out the formalism for performing angular analyses incorporating these higher spin states, from an experimentalist’s perspective. The spin $J \leq 2$ case was addressed in a previous work [2] and subsequently employed to analyze LHCb Run I [3] data in the $\bar{B}^0 \rightarrow K^- \pi^+ \mu^- \mu^+$ mode, with $q^2 \in [1.1, 6.0]$ GeV² and $m_{K\pi} \in [1330, 1530]$ MeV, where S -, P - and D -waves occur in the $[K\pi]$ system. Here $\sqrt{q^2}$ is the invariant di-lepton mass. The interesting feature of the new LHCb data [3] is that it indicates a non-dominant D -wave contribution, contrary to expectations from both existing $\bar{B}^0 \rightarrow J/\psi K^- \pi^+$ [4] and $\bar{B}^0 \rightarrow K^- \pi^+ \gamma$ [5, 6] data and previous theory work [7], where the $K_2^*(1430)$ state plays a dominant role in the $m_{K\pi} \sim 1430$ MeV region. The new results could point toward a revised understanding of the underlying form-factors.

The present paper extends the relevant observables to spin $J \leq 4$, exhausting to a high degree, the known resonant structures listed in the PDG [8]. The motivation to look at these higher spin states is the richer spectrum of angular observables they offer. Belle has already observed the decay $B^- \rightarrow f_2(1270) \ell^- \bar{\nu}_\ell$ [9] while BABAR has probed semileptonic B decays to excited D^{**} states [10]. Even higher spin structures such as $K_4^*(2045)$ [7] are expected to be accessible during the ongoing Run II data-taking period at LHCb.

In addition, we also investigate the issue of the measured angular moments observables not being independent variables. This results in a set of consistency rela-

tions among them. For the $J \leq 2$ case, we provide eight of these relations and validate them against the latest measurements from LHCb [3].

II. THE ANGLE CONVENTIONS

Figure 1a shows the three concerned angles for the prototypical $\bar{B} \rightarrow X \ell_1 \ell_2$ decay, using the $\bar{B}^0 \rightarrow K^- \pi^+ \ell^+ \ell^-$ mode. The hadronic- and leptonic-side helicity angles are θ_V and θ_ℓ , respectively, while χ is the dihedral angle between the hadronic and leptonic decay planes. For three-body decays on the hadronic side, such as $\omega \rightarrow 3\pi$, the normal to the decay plane defines the analyzing direction. Following Ref. [11], in the mother \bar{B} rest frame, the back-to-back leptonic and hadronic systems share a common \hat{y} axis, with opposite \hat{x} and \hat{z} . For the \bar{B} (containing a b -quark) in Fig. 1a, we follow the negatively charged lepton to define the leptonic helicity angle θ_ℓ . The hadronic helicity angle, θ_V is defined similarly. The quadrant of the dihedral angle χ is fixed, by fixing the azimuthal angle of the ℓ^- to be zero in the leptonic helicity frame. The azimuthal angle of the hadronic side analyzer in the hadronic helicity frame then defines χ .

A. CP conjugation

For the CP conjugated decay $B \rightarrow \bar{X} \bar{\ell}_1 \bar{\ell}_2$ in Fig. 1b, we follow the charge-conjugated particles. That is, if we followed the μ^-/K^- for the \bar{B} , we follow the μ^+/K^+ for the B . This is shown in Fig. 1b. The expressions of angular observables in terms of its corresponding amplitudes remain the same during this procedure. However, the amplitudes themselves are related by ¹

$$\mathcal{H}_\lambda^\eta(\delta_W, \delta_S) = \bar{\mathcal{H}}_{-\lambda}^{-\eta}(-\delta_W, \delta_S), \quad (1)$$

¹ The conjugation relations for CP eigenstates $B_{(s)}^0 \rightarrow h^+ h^- \ell^+ \ell^-$ are different and include additional mixing terms.

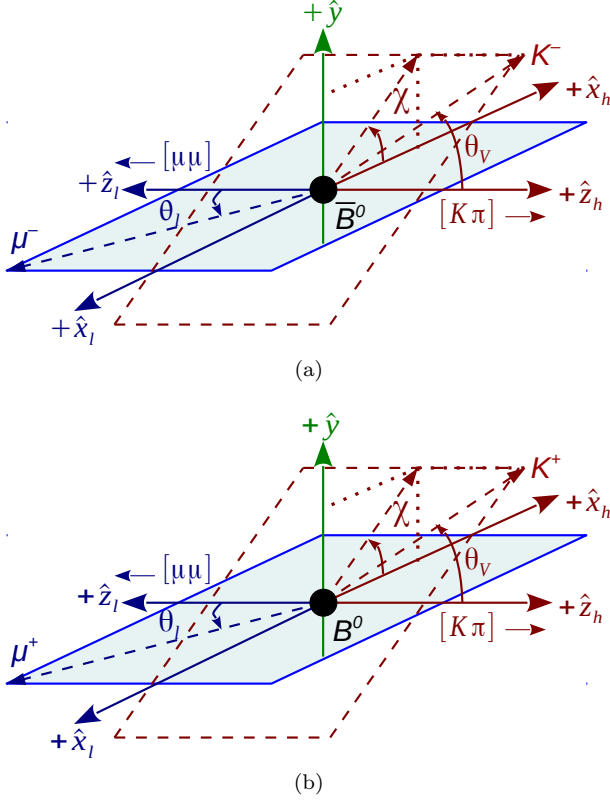


FIG. 1: Angle conventions for the (a) $\bar{B}^0 \rightarrow K^- \pi^+ \mu^- \mu^+$ (b) $B^0 \rightarrow K^+ \pi^- \mu^+ \mu^-$. This serves the prototypical $\bar{B} \rightarrow X \ell_1 \ell_2$ topology in both semileptonic and electroweak penguin analyses. The leptonic and hadronic frames are back-to-back with a common \hat{y} axis.

where $\eta = -1(+1)$ denotes the leptonic-side left(right)-handed amplitudes and $\delta_W(\delta_S)$ are the weak(strong) phases. In the absence of direct CP violation, it can be checked that the measured observables get a sign flip for the terms odd in χ . For convenience, experimentalists flip the sign of χ during the CP conjugation. This way, in the absence of CP violation, the measured observables are the same between the \bar{B} and B decays and one can conveniently merge the two datasets for the CP-averaged measurements.

It is important to note that while reporting the helicity amplitudes, it is pertinent to explicitly mention whether the amplitudes correspond to the \bar{B} or the B . The helicity tags in the amplitudes are dictated by the underlying couplings, and are not convention-dependent. For example, in semileptonic decays the $(V-A)$ structure ensures that $|H_-| > |H_+|$ for the \bar{B} , involving an underlying b -quark transition.

B. Conversion dictionary for semileptonic decays

The three commonly followed theory frameworks for semi-leptonic decays are Gilman-Singleton (GS) [11],

Angle	KS	RB
θ_ℓ	$\pi - \theta_\ell^{\text{GS}}$	θ_ℓ^{GS}
θ_V	θ_V^{GS}	θ_V^{GS}
χ	$\pi + \chi^{\text{GS}}$	$\pi + \chi^{\text{GS}}$

TABLE I: Translation dictionary between GS [11], KS [12] and RB [13] conventions for the semileptonic \bar{B} decay.

Angle	LHCb $\bar{B}^0 \rightarrow \bar{K}^* \mu^- \mu^+$	“Theory”
θ_ℓ	θ_ℓ^{GS}	$\pi - \theta_\ell^{\text{GS}}$
θ_K	θ_V^{GS}	θ_V^{GS}
χ	$-\chi^{\text{GS}}$	χ^{GS}

TABLE II: Translation dictionary between GS [11], LHCb $\bar{B}^0 \rightarrow \bar{K}^* \mu^+ \mu^-$ [14, 15] and “theory” [16] conventions for the electroweak penguin \bar{B} decay. The latest LHCb $\bar{B}^0 \rightarrow K^- \pi^+ \mu^- \mu^+$ [3] paper follows the GS conventions.

Korner-Schuler (KS) [12] and Richman-Burchat (RB) [13]. The charged lepton is always used to define θ_ℓ . We follow the GS convention in this paper, while the KS convention is mostly followed in semi-taonic analyses. The translation between the three angles for the \bar{B} decays is given in Table I.

C. Conversion dictionary for electroweak penguin decays

For electroweak penguins, there are existing LHCb $\bar{B}^0 \rightarrow \bar{K}^* \mu^- \mu^+$ data [14, 15] with one particular convention. The erstwhile theory community [16] used a different convention. The situation is further complicated because, recently, theory papers have appeared [17, 18] that use the LHCb $\bar{B}^0 \rightarrow \bar{K}^* \mu^- \mu^+$ conventions. With reference to Fig. 1, the angle conventions for electroweak penguins are listed in Table II. The negatively charged lepton is used to define θ_ℓ for the \bar{B} decay. We also note that the latest LHCb $\bar{B}^0 \rightarrow K^- \pi^+ \mu^- \mu^+$ [3] paper follows the GS conventions.

III. THE 77 SPIN-4 SPDFG-MOMENTS

For the case where the X_J system comprises spin states till spin $J = 4$, there are 26 complex amplitudes $\{S^\eta, H_\lambda^\eta, D_\lambda^\eta, F_\lambda^\eta, G_\lambda^\eta\}$, where $\eta = \pm 1$ tags the handedness of the leptonic side current, and $\lambda \in \{0, \pm 1\}$ is the helicity of the X_J system. The expressions for the helicity amplitudes in terms of the underlying QCD form-factors and Wilson coefficients can be found in Refs. [2, 7]. The formalism of the moments expansion as in Ref. [2] for the $J \leq 2$ SPD-wave case is easily extended to the $J \leq 4$ SPDFG-wave case. From the F -wave onwards, every higher spin adds 18 moments and there are 77 angular

moments for the spin-4 case. The differential rate is

$$\frac{d\Gamma}{dq^2 d\Omega} = \mathcal{C} \times \left\{ \sum_{i=1}^{77} f_i(\Omega) \Gamma_i(q^2) \right\} \quad (2a)$$

$$\Gamma_i(q^2) = \Gamma_i^L(q^2) + \eta_i^{L \rightarrow R} \Gamma_i^R(q^2), \quad (2b)$$

where the sign $\eta_i^{L \rightarrow R} = \pm 1$ depends on the signature of f_i under $\theta_\ell \rightarrow \pi + \theta_\ell$. The orthonormal angular basis is constructed out of the spherical harmonics $Y_l^m \equiv Y_l^m(\theta_\ell, \chi)$ and the reduced spherical harmonics $P_l^m \equiv \sqrt{2\pi} Y_l^m(\theta_V, 0)$. Following the notation as in Ref. [2], the pre-factor is

$$\mathcal{C} = \frac{\sqrt{8\pi} |V|^2 \mathbf{k} G_F^2 q^2 \mathcal{B}^X}{3m_B^2 (4\pi)^4}, \quad (3)$$

where \mathbf{k} is the breakup momentum if the B meson and \mathcal{B}^X is the branching fraction of the X_J system into the final hadronic states under consideration. For semileptonic $b \rightarrow q\ell^- \bar{\nu}_\ell$ decays, $V \equiv V_{bq}$, while for the electroweak transition $b \rightarrow s\ell^- \ell^+$,

$$V \equiv \left(\frac{\alpha}{2\pi} V_{ts}^* V_{tb} \right). \quad (4)$$

To facilitate the discussion, we first redefine the hadronic-side amplitudes as

$$a = \left(2S - \sqrt{5}D_0 + \frac{9}{4}G_0 \right) \quad (5a)$$

$$b = \left(2\sqrt{3}H_0 - 3\sqrt{7}F_0 \right) \quad (5b)$$

$$c = \left(3\sqrt{5}D_0 - \frac{45}{2}G_0 \right) \quad (5c)$$

$$d = \left(5\sqrt{7}F_0 \right) \quad (5d)$$

$$e = \left(\frac{105}{4}G_0 \right) \quad (5e)$$

$$l_\pm = \mp \left(\sqrt{6}H_\pm - \frac{\sqrt{21}}{2}F_\pm \right) \quad (5f)$$

$$m_\pm = \mp \left(\sqrt{30}D_\pm - \frac{9}{2}\sqrt{5}G_\pm \right) \quad (5g)$$

$$n_\pm = \mp \left(\frac{5\sqrt{21}}{2}F_\pm \right) \quad (5h)$$

$$p_\pm = \mp \left(\frac{21\sqrt{5}}{2}G_\pm \right), \quad (5i)$$

where, for sake of notational simplicity, we have removed the η tag. For what follows, all amplitudes are understood to have an additional η tag.

We next define the set of bilinears $\{\alpha_i, \beta_i^\pm, \delta_i, U_i, V_i, X_i, K_i, L_i, \epsilon_j^\pm, R_j, S_j, T_j, Z_j\}$, where $i \in \{0, \dots, 8\}$ and $j \in \{0, \dots, 7\}$. The expressions for these in terms of the amplitudes are tabulated in App. A. We also define a set of coefficients e_l and s_l to construct the 77 orthonormal

basis moments in Tables III and IV. The numeric values of the e_l and s_l coefficients are also defined in App. B.

Table III lists the 41 moments for the *SPD*-wave case, with additional contributions from the higher waves incorporated now. Table IV lists the additional 36 moments for the *SPDFG* case. The pattern is easily discernable now – from the *F*-wave onwards, each additional higher wave adds 18 angular moments.

IV. CONSISTENCY RELATIONS FOR *SPD*-WAVES

A. The two-component notation

To facilitate the discussion, extending the notation developed in Ref. [19], we define the two-component complex vectors for *S*-, *P*- and *D*-waves for electroweak penguins:

$$\begin{aligned} s &= \begin{pmatrix} S^L \\ S^{R*} \end{pmatrix} \\ h_\parallel &= \begin{pmatrix} H_\parallel^L \\ H_\parallel^{R*} \end{pmatrix} \quad h_\perp = \begin{pmatrix} H_\perp^L \\ -H_\perp^{R*} \end{pmatrix} \quad h_0 = \begin{pmatrix} H_0^L \\ H_0^{R*} \end{pmatrix} \\ d_\parallel &= \begin{pmatrix} D_\parallel^L \\ D_\parallel^{R*} \end{pmatrix} \quad d_\perp = \begin{pmatrix} D_\perp^L \\ -D_\perp^{R*} \end{pmatrix} \quad d_0 = \begin{pmatrix} D_0^L \\ D_0^{R*} \end{pmatrix}. \end{aligned} \quad (6)$$

The $L(R)$ superscripts denote the left(LH)- and right-handed(RH) amplitudes, respectively, and this structure can be continued further to any spin- J . The physical observables will then be constructed out of bilinears formed out of these two component objects.

B. The two-fold ambiguity and the 17 consistency relations

For the charged di-lepton cases, since the final leptonic spins are not measured but averaged over, the full rate is invariant under the following global transformation of each spin- J helicity amplitude:

$$\mathcal{H}_\lambda^{\eta, J} \rightarrow \left(\mathcal{H}_{-\lambda}^{-\eta, J} \right)^*. \quad (7)$$

For the electromagnetic $c\bar{c} \rightarrow \ell^+ \ell^-$ decays, the LH and RH amplitudes are equal and Eq. 7 represents the same two-fold ambiguity as in the determination of β and β_s from $B \rightarrow J/\psi K\pi$ [20] and $B_s \rightarrow J/\psi K K$ [21], respectively.

The effect of this transformation on the two-component vectors in Eq. 6 is that the top and bottom rows get swapped. Therefore, for any pair $\{n_i, n_j\}$ of the two-component vectors, the observable $\mathcal{O}_{ij} \equiv n_i^\dagger n_j$ is invariant under $n_i \rightarrow U n_i$, where the group of symmetry

i	$f_i(\Omega)$	$\Gamma_i^{L,\text{tr}}(q^2)$	$\eta_i^{L \rightarrow R}$
1	$P_0^0 Y_0^0$	$[U_0 + e_{01}U_2 + e_{02}U_4 + e_{03}U_6 + e_{04}U_8]$	$+(L \rightarrow R)$
2	$P_1^0 Y_0^0$	$[e_{10}U_1 + e_{11}U_3 + e_{12}U_5 + e_{13}U_7]$	"
3	$P_2^0 Y_0^0$	$[e_{20}U_2 + e_{21}U_4 + e_{22}U_6 + e_{23}U_8]$	"
4	$P_3^0 Y_0^0$	$[e_{30}U_3 + e_{31}U_5 + e_{32}U_7]$	"
5	$P_4^0 Y_0^0$	$[e_{40}U_4 + e_{41}U_6 + e_{42}U_8]$	"
6	$P_0^0 Y_2^0$	$[V_0 + e_{01}V_2 + e_{02}V_4 + e_{03}V_6 + e_{04}V_8]$	"
7	$P_1^0 Y_2^0$	$[e_{10}V_1 + e_{11}V_3 + e_{12}V_5 + e_{13}V_7]$	"
8	$P_2^0 Y_2^0$	$[e_{20}V_2 + e_{21}V_4 + e_{22}V_6 + e_{23}V_8]$	"
9	$P_3^0 Y_2^0$	$[e_{30}V_3 + e_{31}V_5 + e_{32}V_7]$	"
10	$P_4^0 Y_2^0$	$[e_{40}V_4 + e_{41}V_6 + e_{42}V_8]$	"
11	$P_1^1 \sqrt{2} \text{Re}(Y_2^1)$	$[Z_0 + s_{01}Z_2 + s_{02}Z_4 + s_{03}Z_6]$	"
12	$P_2^1 \sqrt{2} \text{Re}(Y_2^1)$	$[s_{10}Z_1 + s_{11}Z_3 + s_{12}Z_5 + s_{13}Z_7]$	"
13	$P_3^1 \sqrt{2} \text{Re}(Y_2^1)$	$[s_{20}Z_2 + s_{21}Z_4 + s_{22}Z_6]$	"
14	$P_4^1 \sqrt{2} \text{Re}(Y_2^1)$	$[s_{30}Z_3 + s_{31}Z_5 + s_{32}Z_7]$	"
15	$P_1^1 \sqrt{2} \text{Im}(Y_2^1)$	$[S_0 + s_{01}S_2 + s_{02}S_4 + s_{03}S_6]$	"
16	$P_2^1 \sqrt{2} \text{Im}(Y_2^1)$	$[s_{10}S_1 + s_{11}S_3 + s_{12}S_5 + s_{13}S_7]$	"
17	$P_3^1 \sqrt{2} \text{Im}(Y_2^1)$	$[s_{20}S_2 + s_{21}S_4 + s_{22}S_6]$	"
18	$P_4^1 \sqrt{2} \text{Im}(Y_2^1)$	$[s_{30}S_3 + s_{31}S_5 + s_{32}S_7]$	"
19	$P_0^0 \sqrt{2} \text{Re}(Y_2^2)$	$[K_0 + e_{01}K_2 + e_{02}K_4 + e_{03}K_6 + e_{04}K_8]$	"
20	$P_1^0 \sqrt{2} \text{Re}(Y_2^2)$	$[e_{10}K_1 + e_{11}K_3 + e_{12}K_5 + e_{13}K_7]$	"
21	$P_2^0 \sqrt{2} \text{Re}(Y_2^2)$	$[e_{20}K_2 + e_{21}K_4 + e_{22}K_6 + e_{23}K_8]$	"
22	$P_3^0 \sqrt{2} \text{Re}(Y_2^2)$	$[e_{30}K_3 + e_{31}K_5 + e_{32}K_7]$	"
23	$P_4^0 \sqrt{2} \text{Re}(Y_2^2)$	$[e_{40}K_4 + e_{41}K_6 + e_{42}K_8]$	"
24	$P_0^0 \sqrt{2} \text{Im}(Y_2^2)$	$[L_0 + e_{01}L_2 + e_{02}L_4 + e_{03}L_6 + e_{04}L_8]$	"
25	$P_1^0 \sqrt{2} \text{Im}(Y_2^2)$	$[e_{10}L_1 + e_{11}L_3 + e_{12}L_5 + e_{13}L_7]$	"
26	$P_2^0 \sqrt{2} \text{Im}(Y_2^2)$	$[e_{20}L_2 + e_{21}L_4 + e_{22}L_6 + e_{23}L_8]$	"
27	$P_3^0 \sqrt{2} \text{Im}(Y_2^2)$	$[e_{30}L_3 + e_{31}L_5 + e_{32}L_7]$	"
28	$P_4^0 \sqrt{2} \text{Im}(Y_2^2)$	$[e_{40}L_4 + e_{41}L_6 + e_{42}L_8]$	"
29	$P_0^0 Y_1^0$	$[X_0 + e_{01}X_2 + e_{02}X_4 + e_{03}X_6 + e_{04}X_8]$	$-(L \rightarrow R)$
30	$P_1^0 Y_1^0$	$[e_{10}X_1 + e_{11}X_3 + e_{12}X_5 + e_{13}X_7]$	"
31	$P_2^0 Y_1^0$	$[e_{20}X_2 + e_{21}X_4 + e_{22}X_6 + e_{23}X_8]$	"
32	$P_3^0 Y_1^0$	$[e_{30}X_3 + e_{31}X_5 + e_{32}X_7]$	"
33	$P_4^0 Y_1^0$	$[e_{40}X_4 + e_{41}X_6 + e_{42}X_8]$	"
34	$P_1^1 \sqrt{2} \text{Re}(Y_1^1)$	$[R_0 + s_{01}R_2 + s_{02}R_4 + s_{03}R_6]$	"
35	$P_2^1 \sqrt{2} \text{Re}(Y_1^1)$	$[s_{10}R_1 + s_{11}R_3 + s_{12}R_5 + s_{13}R_7]$	"
36	$P_3^1 \sqrt{2} \text{Re}(Y_1^1)$	$[s_{20}R_2 + s_{21}R_4 + s_{22}R_6]$	"
37	$P_4^1 \sqrt{2} \text{Re}(Y_1^1)$	$[s_{30}R_3 + s_{31}R_5 + s_{32}R_7]$	"
38	$P_1^1 \sqrt{2} \text{Im}(Y_1^1)$	$[T_0 + s_{01}T_2 + s_{02}T_4 + s_{03}T_6]$	"
39	$P_2^1 \sqrt{2} \text{Im}(Y_1^1)$	$[s_{10}T_1 + s_{11}T_3 + s_{12}T_5 + s_{13}T_7]$	"
40	$P_3^1 \sqrt{2} \text{Im}(Y_1^1)$	$[s_{20}T_2 + s_{21}T_4 + s_{22}T_6]$	"
41	$P_4^1 \sqrt{2} \text{Im}(Y_1^1)$	$[s_{30}T_3 + s_{31}T_5 + s_{32}T_7]$	"

TABLE III: *SPDFG*-wave moments: the first 41 angular moments corresponding to those for the *SPD*-only case, extended to include *F*- and *G*-wave contributions.

transformation is the group $U(2)$ with $n_{\text{gen}} = 4$ generators and all physical observables allowed in the angular rate expression is of the type \mathcal{O}_{ij} .

For the *SPD*-wave case, with 14 amplitudes, there are $2n_A = 28$ independent real variables and $n_{\text{obs}} = 2n_A - n_{\text{gen}} = 24$ real observables. However, the number of angular moments from Ref. [2] is $n_{\text{mom}} = 41$. Hence, there must be $n_{\text{rel}} = n_{\text{mom}} - n_{\text{obs}} = 17$ relations amongst the 41 observables.

C. The double-basis “trick”

The key towards finding these additional relations is the fact that of the seven $n_i \in \{h_{\parallel}, h_{\perp}, h_0, d_{\parallel}, d_{\perp}, d_0, s\}$ in Eq. 6, any two can be chosen as a basis set and the rest can be expressed as a linear combination. Denoting the basis as $\{n_1, n_2\}$, any other n_i can be written as

$$n_i = a_i n_1 + b_i n_2, \quad (8)$$

i	$f_i(\Omega)$	$\Gamma_i^{L,\text{tr}}(q^2)$	$\eta_i^{L \rightarrow R}$
addition of F -wave			
42	$P_5^0 Y_0^0$	$[e_{50}U_5 + e_{51}U_7]$	$+(L \rightarrow R)$
43	$P_6^0 Y_0^0$	$[e_{60}U_6 + e_{61}U_8]$	"
44	$P_5^0 Y_2^0$	$[e_{50}V_5 + e_{51}V_7]$	"
45	$P_6^0 Y_2^0$	$[e_{60}V_6 + e_{61}V_8]$	"
46	$P_5^1 \sqrt{2} \text{Re}(Y_2^1)$	$[s_{40}Z_4 + s_{41}Z_6]$	"
47	$P_6^1 \sqrt{2} \text{Re}(Y_2^1)$	$[s_{50}Z_5 + s_{51}Z_7]$	"
48	$P_5^1 \sqrt{2} \text{Im}(Y_2^1)$	$[s_{40}S_4 + s_{41}S_6]$	"
49	$P_6^1 \sqrt{2} \text{Im}(Y_2^1)$	$[s_{50}S_5 + s_{51}S_7]$	"
50	$P_5^0 \sqrt{2} \text{Re}(Y_2^2)$	$[e_{50}K_5 + e_{51}K_7]$	"
51	$P_6^0 \sqrt{2} \text{Re}(Y_2^2)$	$[e_{60}K_6 + e_{61}K_8]$	"
52	$P_5^0 \sqrt{2} \text{Im}(Y_2^2)$	$[e_{50}L_5 + e_{51}L_7]$	"
53	$P_6^0 \sqrt{2} \text{Im}(Y_2^2)$	$[e_{60}L_6 + e_{61}L_8]$	"
54	$P_5^0 Y_1^0$	$[e_{50}X_5 + e_{51}X_7]$	$-(L \rightarrow R)$
55	$P_6^0 Y_1^0$	$[e_{60}X_6 + e_{61}X_8]$	"
56	$P_5^1 \sqrt{2} \text{Re}(Y_1^1)$	$[s_{40}R_4 + s_{41}R_6]$	"
57	$P_6^1 \sqrt{2} \text{Re}(Y_1^1)$	$[s_{50}R_5 + s_{51}R_7]$	"
58	$P_5^1 \sqrt{2} \text{Im}(Y_1^1)$	$[s_{40}T_4 + s_{41}T_6]$	"
59	$P_6^1 \sqrt{2} \text{Im}(Y_1^1)$	$[s_{50}T_5 + s_{51}T_7]$	"
addition of G -wave			
60	$P_7^0 Y_0^0$	$e_7 U_7$	$+(L \rightarrow R)$
61	$P_8^0 Y_0^0$	$e_8 U_8$	"
62	$P_7^0 Y_2^0$	$e_7 V_7$	"
63	$P_8^0 Y_2^0$	$e_8 V_8$	"
64	$P_7^1 \sqrt{2} \text{Re}(Y_2^1)$	$s_{61} Z_6$	"
65	$P_8^1 \sqrt{2} \text{Re}(Y_2^1)$	$s_7 Z_7$	"
66	$P_7^1 \sqrt{2} \text{Im}(Y_2^1)$	$e_7 L_7$	"
67	$P_8^1 \sqrt{2} \text{Im}(Y_2^1)$	$e_8 L_8$	"
68	$P_7^0 \sqrt{2} \text{Re}(Y_2^2)$	$e_7 K_7$	"
69	$P_8^0 \sqrt{2} \text{Re}(Y_2^2)$	$e_8 K_8$	"
70	$P_7^0 \sqrt{2} \text{Im}(Y_2^2)$	$e_7 L_7$	"
71	$P_8^0 \sqrt{2} \text{Im}(Y_2^2)$	$e_8 L_8$	"
72	$P_7^0 Y_1^0$	$e_7 X_7$	$-(L \rightarrow R)$
73	$P_8^0 Y_1^0$	$e_8 X_8$	"
74	$P_7^1 \sqrt{2} \text{Re}(Y_1^1)$	$s_{61} R_6$	"
75	$P_8^1 \sqrt{2} \text{Re}(Y_1^1)$	$s_7 R_7$	"
76	$P_7^1 \sqrt{2} \text{Im}(Y_1^1)$	$s_{61} T_6$	"
77	$P_8^1 \sqrt{2} \text{Im}(Y_1^1)$	$s_7 T_7$	"

TABLE IV: $SPDFG$ -wave moments: the 18 + 18 set of additional moments over those in Table III for the SPD case.

where the coefficients a_i , b_i can be solved as [19]

$$a_i = \frac{|n_2|^2(n_1^\dagger n_i) - (n_1^\dagger n_2)(n_2^\dagger n_i)}{|n_1|^2|n_2|^2 - |n_1^\dagger n_2|^2} \quad (9)$$

$$b_i = \frac{|n_1|^2(n_2^\dagger n_i) - (n_2^\dagger n_1)(n_1^\dagger n_i)}{|n_1|^2|n_2|^2 - |n_1^\dagger n_2|^2} \quad (10)$$

Thus we have 5 real equations:

$$|n_i|^2 = a_i(n_i^\dagger n_1) + b_i(n_i^\dagger n_2), \quad i \in \{3, \dots, 7\} \quad (11)$$

and ${}^5C_2 = 10$ complex equations:

$$n_i^\dagger n_j = a_j(n_i^\dagger n_1) + b_j(n_i^\dagger n_2), \quad i, j \in \{3, \dots, 7\} \quad (12)$$

If one had expressions of all the relevant $\text{Re}(n_i^\dagger n_j)$ and $\text{Im}(n_i^\dagger n_j)$ in terms of the observables, the above sets of equations would yield all the relations.

For the pure P -wave case, the number of independent observables is 8 and all the combinations $n_i^\dagger n_j$ can be solved out in terms of the observables [19]. For the SP -wave case, there are 12 independent observables. Even here, the combination $\text{Im}(n_S^\dagger n_0)$ is not given in terms of any of the angular observables. It is fortuitous that this combination is not needed to solve for the relations. The minimal set of the 12 independent observables for the SP -wave case was given in Ref. [19].

For the SPD -wave case, the situation is completely different, and many of the $n_i^\dagger n_j$ combinations remain unsolvable in terms of the observables.

D. Solving for the bilinears

For the SPD -wave case, we list below the known set of bilinears that can be expressed in terms of the 41 Γ_i

moments observables in Ref. [2]:

$$|d_0|^2 = \frac{7}{9} \left(\frac{\Gamma_5}{2} - \sqrt{5}\Gamma_{10} \right) \quad (13.1)$$

$$|d_{\parallel}|^2 = \frac{7}{4} \left(\sqrt{\frac{5}{3}}\Gamma_{23} - \frac{1}{3} \left(\sqrt{5}\Gamma_{10} + \Gamma_5 \right) \right) \quad (13.2)$$

$$|d_{\perp}|^2 = \frac{7}{4} \left(-\sqrt{\frac{5}{3}}\Gamma_{23} - \frac{1}{3} \left(\sqrt{5}\Gamma_{10} + \Gamma_5 \right) \right) \quad (13.3)$$

$$|h_{\parallel}|^2 = \frac{1}{2} \left[\frac{2}{3} \left(\Gamma_1 + \sqrt{5}\Gamma_6 \right) + \frac{7}{6} \left(\sqrt{5}\Gamma_{10} + \Gamma_5 \right) - \sqrt{\frac{5}{3}} \left(2\Gamma_{19} + \frac{7}{2}\Gamma_{23} \right) \right] \quad (13.4)$$

$$|h_{\perp}|^2 = \frac{1}{2} \left[\frac{2}{3} \left(\Gamma_1 + \sqrt{5}\Gamma_6 \right) + \frac{7}{6} \left(\sqrt{5}\Gamma_{10} + \Gamma_5 \right) + \sqrt{\frac{5}{3}} \left(2\Gamma_{19} + \frac{7}{2}\Gamma_{23} \right) \right] \quad (13.5)$$

$$Re(d_{\parallel}^{\dagger} h_{\parallel}) = \frac{5}{6} \left[\frac{1}{\sqrt{3}} \left(\frac{\Gamma_2}{\sqrt{5}} + \Gamma_7 \right) - \Gamma_{20} \right] \quad (13.6)$$

$$Re(d_{\perp}^{\dagger} h_{\perp}) = \frac{5}{6} \left[\frac{1}{\sqrt{3}} \left(\frac{\Gamma_2}{\sqrt{5}} + \Gamma_7 \right) + \Gamma_{20} \right] \quad (13.7)$$

$$Re(d_0^{\dagger} h_0) = \frac{1}{3\sqrt{3}} \left[\frac{\sqrt{35}}{2}\Gamma_4 + \frac{5}{\sqrt{3}} \left(\Gamma_7 + \frac{\Gamma_2}{\sqrt{5}} \right) \right] \quad (13.8)$$

$$Re(h_0^{\dagger} s) = -\frac{1}{18}\Gamma_2 - \frac{\sqrt{21}}{9}\Gamma_4 - \frac{5\sqrt{5}}{9}\Gamma_7 \quad (13.9)$$

$$Re(h_{\parallel}^{\dagger} h_{\perp}) = \frac{5}{12} \left(-\frac{\Gamma_{29}}{\sqrt{3}} + \frac{7}{\sqrt{15}}\Gamma_{31} \right) \quad (13.10)$$

$$Im(h_{\parallel}^{\dagger} h_{\perp}) = \frac{5}{12\sqrt{3}} \left(\sqrt{5}\Gamma_{24} - 7\Gamma_{26} \right) \quad (13.11)$$

$$Re(d_{\parallel}^{\dagger} d_{\perp}) = -\frac{7}{12\sqrt{3}} \left(\Gamma_{29} + \sqrt{5}\Gamma_{31} \right) \quad (13.12)$$

$$Im(d_{\parallel}^{\dagger} d_{\perp}) = \frac{7}{12} \sqrt{\frac{5}{3}} \left(\Gamma_{24} + \sqrt{5}\Gamma_{26} \right) \quad (13.13)$$

$$Re(d_0^{\dagger} d_{\parallel}) = -\frac{7\sqrt{2}}{6}\Gamma_{14} \quad (13.14)$$

$$Im(d_0^{\dagger} d_{\parallel}) = -\frac{7}{3\sqrt{10}}\Gamma_{41} \quad (13.15)$$

$$Re(d_0^{\dagger} d_{\perp}) = \frac{7}{3\sqrt{10}}\Gamma_{37} \quad (13.16)$$

$$Im(d_0^{\dagger} d_{\perp}) = \frac{7\sqrt{2}}{6}\Gamma_{18} \quad (13.17)$$

In particular $(|h_0|^2 + \sqrt{5}Re(d_0^{\dagger} s))$ occurs together, so $|h_0|^2$ can not be extracted. Also, $(|h_0|^2 + |s|^2)$ occurs together, so F_S can not be extracted. The D -wave fraction

$$F_D = (|d_0|^2 + |d_{\perp}|^2 + |d_{\parallel}|^2)/\Gamma_1 \quad (14)$$

is completely extractable however.

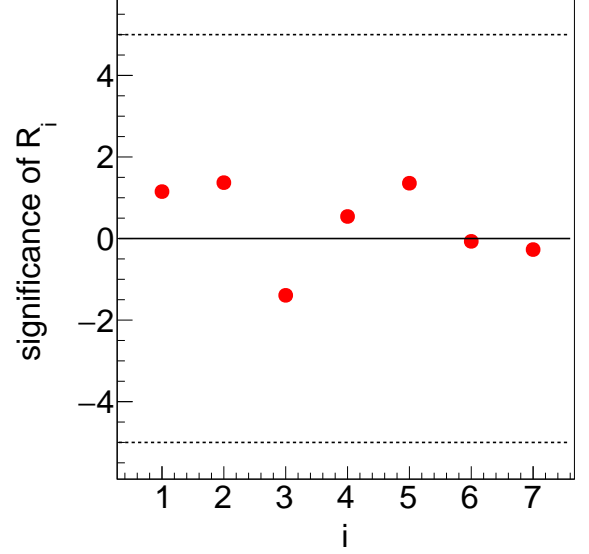


FIG. 2: The significance of the seven R_i observables defined in Eq. 15, integrated over the range $q^2 \in [1.1, 6.0]$ GeV² and $m_{K\pi} \in [1330, 1530]$ MeV, as measured by LHCb in the mode $\bar{B}^0 \rightarrow K^- \pi^+ \mu^- \mu^+$ [3]. No significant deviation from zero is seen, pointing to the internal consistency among the measurements.

E. Relations among the observables

We first list the 7 linear relations below:

$$0 = R_1 \equiv \Gamma_{25} + \sqrt{\frac{7}{3}}\Gamma_{27} \quad (15.1)$$

$$0 = R_2 \equiv \Gamma_{20} + \sqrt{\frac{7}{3}}\Gamma_{22} \quad (15.2)$$

$$0 = R_3 \equiv \sqrt{\frac{3}{7}}\Gamma_{30} + \Gamma_{32} \quad (15.3)$$

$$0 = R_4 \equiv \frac{1}{\sqrt{5}} (3\Gamma_{23} + \Gamma_{19}) + \Gamma_{21} \quad (15.4)$$

$$0 = R_5 \equiv \frac{\Gamma_3}{\sqrt{5}} + \Gamma_8 + \frac{3}{5} \left[(\sqrt{5}\Gamma_{10} + \Gamma_5) + \frac{1}{3}(\Gamma_1 + \sqrt{5}\Gamma_6) \right] \quad (15.5)$$

$$0 = R_6 \equiv 3\Gamma_{28} + (\Gamma_{24} + \sqrt{5}\Gamma_{26}) \quad (15.6)$$

$$0 = R_7 \equiv 3\Gamma_{33} + (\Gamma_{29} + \sqrt{5}\Gamma_{31}), \quad (15.7)$$

where the R_i 's can be taken as new observables as functions of q^2 and m_X whose measured values are expected to be zero. A useful consistency check is therefore that the experimental data show no significant deviation from zero in these observables. Figure 2 shows the experimentally measured significance (measured value divided by its uncertainty) from LHCb [3] of the seven R_i observables integrated over the q^2 range $[1.1, 6.0]$ GeV² and $m_{K\pi}$ range $[1330, 1530]$ MeV in the mode $\bar{B}^0 \rightarrow$

$K^-\pi^+\mu^-\mu^+$. All seven R_i observables are found consistent with zero.

Next, we employ the method elaborated in Sec. IV C

using the basis $\{d_0, d_\perp\}$ and $n_i = d_\parallel$. This yields the following relation:

$$0 = R_8 \equiv \left[\left(\sqrt{\frac{5}{3}}\Gamma_{23} + \frac{\sqrt{5}\Gamma_{10} + \Gamma_5}{3} \right) \left(\Gamma_{14}^2 + \frac{\Gamma_{41}^2}{5} \right) - \left(\frac{\Gamma_5/2 - \sqrt{5}\Gamma_{10}}{54} \right) \left((\Gamma_{29} + \sqrt{5}\Gamma_{31})^2 + 5(\Gamma_{24} + \sqrt{5}\Gamma_{26})^2 \right) \right] \\ + \frac{2}{3\sqrt{15}} \left[(\Gamma_{37}\Gamma_{14} + \Gamma_{18}\Gamma_{41}) (\Gamma_{29} + \sqrt{5}\Gamma_{31}) + (\Gamma_{37}\Gamma_{41} - 5\Gamma_{18}\Gamma_{14}) (\Gamma_{24} + \sqrt{5}\Gamma_{26}) \right] \\ - \left(\sqrt{\frac{5}{3}}\Gamma_{23} - \frac{\sqrt{5}\Gamma_{10} + \Gamma_5}{3} \right) \left[\left(\frac{\Gamma_5/2 - \sqrt{5}\Gamma_{10}}{2} \right) \left(\sqrt{\frac{5}{3}}\Gamma_{23} + \frac{\sqrt{5}\Gamma_{10} + \Gamma_5}{3} \right) + \left(\frac{\Gamma_{37}^2}{5} + \Gamma_{18}^2 \right) \right] \quad (16)$$

Since this relation is non-linear, it is not possible to validate this from experimentally measured binned observables Γ_i that are integrated over a given q^2 and m_X range. Within the triplet, $\{d_0, d_\perp, d_\parallel\}$, we have also checked that all other combinations yield no new relation.

V. CONCLUSIONS

In conclusion, we have presented the the first full angular moments expansion for semileptonic and electroweak penguin $\bar{B} \rightarrow X_J \ell_1 \ell_2$ decays, where the X_J system can be in a spin $J \leq 4$ state. This will enable angular analyses of even higher spin states towards New Physics searches incorporating these new excited modes. We expect this method to be directly employed in Run II analyses at LHCb. Further applications can include $\bar{B} \rightarrow \pi\pi\ell^-\bar{\nu}_\ell$ over a wide $m_{\pi\pi}$ kinematic regime at Belle II, for extracting $|V_{ub}|$ and right-handed current searches. The method can also be used to directly probe the spin content of excited D^{**} states in exclusive $\bar{B} \rightarrow D^{**}\ell^-\bar{\nu}_\ell$ topologies towards reconciling the existing gap between inclusive and exclusive $\bar{B} \rightarrow X_c\ell^-\bar{\nu}_\ell$ branching fractions [22].

The formalism also allows for internal consistency checks, since the moments are not independent observables. In this paper we also validated the available consistency checks for the latest LHCb analysis [3] involving S -, P - and D -waves.

Acknowledgments

We thank Quim Matias for helpful discussions on the two-component notation and derivations of the consistency relations.

Appendix A: Bilinear variables for the expansion

We list here the definitions of the various bilinears in terms of the amplitudes given by Eq. 5.

$$\alpha_0 = (|a|^2) \quad (A1a)$$

$$\alpha_1 = (ab^* + ba^*) \quad (A1b)$$

$$\alpha_2 = (ac^* + ca^* + |b|^2) \quad (A1c)$$

$$\alpha_3 = (ad^* + da^* + bc^* + cb^*) \quad (A1d)$$

$$\alpha_4 = (ae^* + a^*e + bd^* + d^*b + |c|^2) \quad (A1e)$$

$$\alpha_5 = (be^* + eb^* + cd^* + dc^*) \quad (A1f)$$

$$\alpha_6 = (ce^* + ec^* + |d|^2) \quad (A1g)$$

$$\alpha_7 = (ed^* + e^*d) \quad (A1h)$$

$$\alpha_8 = (|e|^2) \quad (A1i)$$

$$\delta_0 = (l_+ l_-^*) \quad (A2a)$$

$$\delta_1 = (l_+ m_-^* + m_+ l_-^*) \quad (A2b)$$

$$\delta_2 = (l_+ n_-^* + n_+ l_-^* + m_+ m_-^* - l_+ l_-^*) \quad (A2c)$$

$$\delta_3 = (l_+ p_-^* + p_+ l_-^* + m_+ n_-^* + n_+ m_-^* - (l_+ m_-^* + m_+ l_-^*)) \quad (A2d)$$

$$\delta_4 = (m_+ p_-^* + p_+ m_-^* + n_+ n_-^* - (l_+ n_-^* + n_+ l_-^* + m_+ m_-^*)) \quad (A2e)$$

$$\delta_5 = (n_+ p_-^* + p_+ n_-^* - (l_+ p_-^* + p_+ l_-^* + m_+ n_-^* + n_+ m_-^*)) \quad (A2f)$$

$$\delta_6 = (p_+ p_-^* - (m_+ p_-^* + p_+ m_-^* + n_+ n_-^*)) \quad (A2g)$$

$$\delta_7 = -(n_+ p_-^* + p_+ n_-^*) \quad (A2h)$$

$$\delta_8 = -(p_+ p_-^*) \quad (A2i)$$

Appendix B: The numeric coefficients

$$\begin{aligned}
\beta_0^\pm &= (|l_\pm|^2) & (A3a) \\
\beta_1^\pm &= (l_\pm m_\pm^* + l_\pm^* m_\pm) & (A3b) \\
\beta_2^\pm &= (l_\pm n_\pm^* + l_\pm^* n_\pm + |m_\pm|^2 - |l_\pm|^2) & (A3c) \\
\beta_3^\pm &= (l_\pm p_\pm^* + l_\pm^* p_\pm + m_\pm n_\pm^* + m_\pm^* n_\pm - (l_\pm m_\pm^* + l_\pm^* m_\pm)) & (A3d) \\
\beta_4^\pm &= (m_\pm p_\pm^* + m_\pm^* p_\pm + |n_\pm|^2 - (l_\pm n_\pm^* + l_\pm^* n_\pm + |m_\pm|^2)) & (A3e) \\
\beta_5^\pm &= (n_\pm p_\pm^* + n_\pm^* p_\pm - (l_\pm p_\pm^* + l_\pm^* p_\pm + m_\pm n_\pm^* + m_\pm^* n_\pm)) & (A3f) \\
\beta_6^\pm &= (|p_\pm|^2 - (m_\pm p_\pm^* + m_\pm^* p_\pm + |n_\pm|^2)) & (A3g) \\
\beta_7^\pm &= -(n_\pm p_\pm^* + n_\pm^* p_\pm) & (A3h) \\
\beta_8^\pm &= -(|p_\pm|^2) & (A3i)
\end{aligned}$$

$$\begin{aligned}
\epsilon_0^\pm &= (l_\pm a^*) & (A4a) \\
\epsilon_1^\pm &= (l_\pm b^* + m_\pm a^*) & (A4b) \\
\epsilon_2^\pm &= (l_\pm c^* + n_\pm a^* + m_\pm b^*) & (A4c) \\
\epsilon_3^\pm &= (l_\pm d^* + p_\pm a^* + m_\pm c^* + n_\pm b^*) & (A4d) \\
\epsilon_4^\pm &= (m_\pm d^* + p_\pm b^* + l_\pm e^* + n_\pm c^*) & (A4e) \\
\epsilon_5^\pm &= (m_\pm e^* + n_\pm d^* + p_\pm c^*) & (A4f) \\
\epsilon_6^\pm &= (n_\pm e^* + p_\pm d^*) & (A4g) \\
\epsilon_7^\pm &= (p_\pm e^*) & (A4h)
\end{aligned}$$

These are used to further define the following combinations

$$U_i = \frac{\alpha_i + \beta_i^+ + \beta_i^-}{4} \quad (A5a)$$

$$V_i = \frac{\beta_i^+ + \beta_i^- - 2\alpha_i}{8\sqrt{5}} \quad (A5b)$$

$$X_i = -\frac{\sqrt{3}}{8}(\beta_i^+ - \beta_i^-) \quad (A5c)$$

$$K_i = \frac{1}{4}\sqrt{\frac{3}{5}} \text{Re}(\delta_i) \quad (A5d)$$

$$L_i = -\frac{1}{4}\sqrt{\frac{3}{5}} \text{Im}(\delta_i) \quad (A5e)$$

$$R_j = -\frac{\text{Re}(\epsilon_j^+ + \epsilon_j^-)}{4} \quad (A5f)$$

$$S_j = -\frac{\text{Im}(\epsilon_j^+ + \epsilon_j^-)}{4\sqrt{5}} \quad (A5g)$$

$$T_j = \frac{\text{Im}(\epsilon_j^+ - \epsilon_j^-)}{4} \quad (A5h)$$

$$Z_j = \frac{\text{Re}(\epsilon_j^+ - \epsilon_j^-)}{4\sqrt{5}}, \quad (A5i)$$

for $i \in \{0, \dots, 8\}$ and $j \in \{0, \dots, 7\}$, that are employed in the definition of the moments in Tables III and IV.

Next, we define the coefficients e_l and s_l :

$$e_{01} = \frac{1}{3} \quad s_{01} = \frac{1}{5} \quad (B1a)$$

$$e_{02} = \frac{1}{5} \quad s_{02} = \frac{3}{35} \quad (B1b)$$

$$e_{03} = \frac{1}{7} \quad s_{03} = \frac{1}{21} \quad (B1c)$$

$$e_{04} = \frac{1}{9} \quad (B1d)$$

$$e_{10} = \frac{1}{\sqrt{3}} \quad s_{10} = \frac{1}{\sqrt{5}} \quad (B1e)$$

$$e_{11} = \frac{\sqrt{3}}{5} \quad s_{11} = \frac{3}{7\sqrt{5}} \quad (B1f)$$

$$e_{12} = \frac{\sqrt{3}}{7} \quad s_{12} = \frac{\sqrt{5}}{21} \quad (B1g)$$

$$e_{13} = \frac{1}{3\sqrt{3}} \quad s_{13} = \frac{\sqrt{5}}{33} \quad (B1h)$$

$$e_{20} = \frac{2}{3\sqrt{5}} \quad s_{20} = \frac{2\sqrt{2}}{5\sqrt{7}} \quad (B1i)$$

$$e_{21} = \frac{4}{7\sqrt{5}} \quad s_{21} = \frac{4\sqrt{2}}{15\sqrt{7}} \quad (B1j)$$

$$e_{22} = \frac{10}{21\sqrt{5}} \quad s_{22} = \frac{2\sqrt{2}}{11\sqrt{7}} \quad (B1k)$$

$$e_{23} = \frac{40}{99\sqrt{5}} \quad (B1l)$$

$$e_{30} = \frac{2}{5\sqrt{7}} \quad s_{30} = \frac{2\sqrt{2}}{7\sqrt{15}} \quad (B1m)$$

$$e_{31} = \frac{4}{9\sqrt{7}} \quad s_{31} = \frac{4\sqrt{10}}{77\sqrt{3}} \quad (B1n)$$

$$e_{32} = \frac{2\sqrt{7}}{33} \quad s_{32} = \frac{2\sqrt{30}}{143} \quad (B1o)$$

$$e_{40} = \frac{8}{105} \quad s_{40} = \frac{8}{21\sqrt{55}} \quad (B1p)$$

$$e_{41} = \frac{8}{77} \quad s_{41} = \frac{8\sqrt{5}}{91\sqrt{11}} \quad (B1q)$$

$$e_{42} = \frac{16}{143} \quad (B1r)$$

$$e_{50} = \frac{8}{63\sqrt{11}} \quad s_{50} = \frac{8}{33\sqrt{91}} \quad (B1s)$$

$$e_{51} = \frac{8}{39\sqrt{11}} \quad s_{51} = \frac{8\sqrt{7}}{165\sqrt{13}} \quad (B1t)$$

$$e_{60} = \frac{16}{231\sqrt{13}} \quad s_{61} = \frac{32}{429\sqrt{35}} \quad (B1u)$$

$$e_{61} = \frac{64}{495\sqrt{13}} \quad s_7 = \frac{32}{715\sqrt{51}} \quad (B1v)$$

$$e_7 = \frac{16}{429\sqrt{15}} \quad (B1w)$$

$$e_8 = \frac{128}{6435\sqrt{17}} \quad (B1x)$$

-
- [1] R. Aaij et al. (LHCb collaboration), JHEP **02**, 104 (2016), 1512.04442.
 - [2] B. Dey, Phys. Rev. **D92**, 033013 (2015), 1505.02873.
 - [3] R. Aaij et al. (LHCb) (2016), 1609.04736.
 - [4] K. Chilikin et al. (Belle collaboration), Phys. Rev. **D90**, 112009 (2014), 1408.6457.
 - [5] S. Nishida et al. (Belle), Phys. Rev. Lett. **89**, 231801 (2002), hep-ex/0205025.
 - [6] B. Aubert et al. (BaBar), Phys. Rev. **D70**, 091105 (2004), hep-ex/0409035.
 - [7] C.-D. Lu and W. Wang, Phys. Rev. **D85**, 034014 (2012), 1111.1513.
 - [8] K. A. Olive et al. (Particle Data Group), Chin. Phys. **C38**, 090001 (2014).
 - [9] A. Sibidanov et al. (Belle), Phys. Rev. **D88**, 032005 (2013), 1306.2781.
 - [10] J. P. Lees et al. (BaBar), Phys. Rev. Lett. **116**, 041801 (2016), 1507.08303.
 - [11] F. J. Gilman and R. L. Singleton, Phys. Rev. **D41**, 142 (1990).
 - [12] J. G. Korner and G. A. Schuler, Z. Phys. **C46**, 93 (1990).
 - [13] J. D. Richman and P. R. Burchat, Rev. Mod. Phys. **67**, 893 (1995), hep-ph/9508250.
 - [14] R. Aaij et al. (LHCb), JHEP **08**, 131 (2013), 1304.6325.
 - [15] R. Aaij et al. (LHCb), JHEP **02**, 104 (2016), 1512.04442.
 - [16] U. Egede, T. Hurth, J. Matias, M. Ramon, and W. Reece, JHEP **10**, 056 (2010), 1005.0571.
 - [17] D. Becirevic, O. Sumensari, and R. Zukanovich Funchal, Eur. Phys. J. **C76**, 134 (2016), 1602.00881.
 - [18] J. Gratrex, M. Hopfer, and R. Zwicky, Phys. Rev. **D93**, 054008 (2016), 1506.03970.
 - [19] L. Hofer and J. Matias, JHEP **09**, 104 (2015), 1502.00920.
 - [20] B. Aubert et al. (BaBar), Phys. Rev. **D71**, 032005 (2005), hep-ex/0411016.
 - [21] R. Aaij et al. (LHCb), Phys. Rev. Lett. **114**, 041801 (2015), 1411.3104.
 - [22] F. U. Bernlochner, Z. Ligeti, and S. Turczyk, Phys. Rev. **D85**, 094033 (2012), 1202.1834.